ImmunoHorizons

RESEARCH ARTICLE

Adaptive Immunity

PD-1 Limits IL-2 Production and Thymic Regulatory T Cell Development

Breanna Caruso,* Benjamin R. Weeder,† Reid F. Thompson,†,‡,§,¶ and Amy E. Moran*,‡

*Cell, Developmental and Cancer Biology, Oregon Health and Science University, Portland, OR;†Department of Biomedical Engineering, Oregon Health and Science University, Portland, OR;‡Knight Cancer Institute, Oregon Health and Science University, Portland, OR;§Department of Radiation Medicine, Oregon Health and Science University, Portland, OR; and ¶Veterans Affairs Portland Health Care System, Portland,OR

ABSTRACT

Inhibitory proteins, such as programmed cell death protein 1 (PD-1), have been studied extensively in peripheral T cell responses to foreign Ags, self-Ags, and neoantigens. Notably, these proteins are first expressed during T cell development in the thymus. Reports suggest that PD-1 limits regulatory T cell (Treg) development, but the mechanism by which PD-1 exerts this function remains unknown. The present study expands the evaluation of murine PD-1 and its ligands in the thymus, demonstrating that some of the highest expressers of PD-1 and programmed death-ligand 1 are agonist selected cells. Surprisingly, we reveal a selective role for PD-1 in regulating the developmental niche only for Tregs because other agonist selected cell populations, such as NK T cells, remain unchanged. We also ruled out PD-1 as a regulator of proliferation or cell death of agonist selected Tregs and further demonstrated that PD-1–deficient Tregs have reduced TCR signaling. Unexpectedly, the data suggest that PD-1–deficient thymocytes produce elevated levels of IL-2, a Treg niche–limiting cytokine. Collectively, these data suggest a novel role for PD-1 in regulating IL-2 production and the concurrent agonist selection of murine thymic Tregs. This observation has implications for the use of checkpoint blockade in the context of cancer and infection. *ImmunoHorizons*, 2024, 8: 281–294.

INTRODUCTION

The thymus is critical in establishing and maintaining a diverse peripheral T cell pool capable of mounting an effective response against a variety of immunologic insults. This diversity is largely due to rearrangement of germline TCR genes, which generate T cells that have a broad range of specificities. Thymocytes interact with ligands presented on self-MHC molecules in the cortex, and those with productive TCRs will receive survival signals necessary for continued maturation in the process of positive selection. Developing thymocytes are then queried for self-reactivity in the medulla, and those that receive strong TCR signals in response to self-ligands are deleted in the process of negative selection. A portion of cells that demonstrate some reactivity to self-ligands are diverted into alternative lineages in the process of agonist selection to produce NK T cells (NKT), γδ T cells, CD8αα T cells, or regulatory T cells (Tregs) (1).

Received for publication November 21, 2023. Accepted for publication November 22, 2023.

Address correspondence and reprint requests to: Dr. Amy E. Moran, Oregon Health and Science University, 3181 S.W. Sam Jackson Park Road, Mail Code KR-CDCB, Portland, OR 97239-3098. E-mail address: moranam@ohsu.edu

ORCIDs: 0000-0002-1519-8131 (B.C.); 0000-0003-1952-7737 (A.E.M.).

This work was supported by Grants National Science Foundation AVPRS0015, National Institutes of Health/National Cancer Institute R37CA263592, and National Institutes of Health F31CA261058 and the Oregon Health & Science University Foundation.

A.E.M. conceived the study with B.C. B.C. and A.E.M. designed the experiments. B.C. performed all the experiments and analyzed the data. Single-cell data analysis was performed by B.R.W. with guidance from R.F.T. For all other experiments, B.C. and A.E.M. interpreted the data. B.C., B.R.W, and A.E.M. wrote the manuscript.

The sequencing data presented in this article have been submitted to the Gene Expression Omnibus database (https://www.ncbi.nlm.nih.gov/geo/query/acc.cgi?acc=GSE255727) under accession number GSE255727.

Abbreviations used in this article: CTEC, cortical thymic epithelial cell; DEG, differentially expressed gene; DN, double-negative; gMFI, geometric mean fluorescence intensity; GSEA, gene set enrichment analysis; mTEC, medullary thymic epithelial cell; PD-1, programmed cell death protein 1; PD-L1, programmed death-ligand 1; scRNAseq, single-cell RNA sequencing; TEC, thymic epithelial cell; Treg, regulatory T cell; WT, wild type.

The online version of this article contains supplemental material.

This article is distributed under the terms of the CC BY-NC 4.0 Unported license.

Copyright © 2024 The Authors

Costimulatory and coinhibitory molecules affect cell fate decisions in the thymus by enhancing or dampening signaling through the TCR. The most well-characterized pathway involves CD80/CD86 (B7-1/B7-2) ligands that bind to and activate CD28 and CTLA-4. Signaling through CD28 serves to enhance TCR signaling, whereas CTLA-4 dampens TCR signaling (2). The B7 family has expanded to include programmed cell death protein 1 (PD-1) (3), which is a CD28 homolog containing inhibitory motifs in its cytoplasmic tail that recruit Src homology region 2 domain-containing phosphatase (SHP)-1 and SHP-2 upon engagement with its ligands (4), programmed death-ligand 1 (PD-L1) (5), and PD-L2 (6). This leads to dephosphorylation of signaling molecules downstream of TCR (7) and CD28 (8). The importance of the PD-1–inhibitory signal is demonstrated by the phenotype of PD-1–deficient (PD-1$^{-/-}$) mice: C57BL/6 PD-1$^{-/-}$ mice display features of lupus (9), and BALB/c PD-1$^{-/-}$ mice develop a cardiomyopathy (10). Together, these observations establish a role for PD-1 in regulating tolerance; however, it is notable that loss of this inhibitory protein does not result in more widespread autoimmunity.

Because costimulation and coinhibition are known to modify TCR signaling, it stands to reason that these pathways may also regulate thymocyte selection. Studies have shown that PD-1 is expressed by developing thymocytes (11). Furthermore, PD-L1 is expressed throughout the thymus, whereas PD-L2 is limited to medullary stromal cells (12). Notably, the expression of both PD-L1 and PD-L2 by medullary stromal cells overlaps with Aire^{+} medullary thymic epithelial cells (TECs) that mediate negative and/or agonist selection (13, 14). Some of the first studies to implicate PD-1 in T cell development were derived from PD-1$^{-/-}$ TCR transgenic mice, which revealed a role for PD-1 in facilitating TCRβ selection and inhibiting positive selection (15, 16). Further studies have suggested that PD-1$^{-/-}$ cells are more likely to become Tregs in the thymus (17, 18), pointing to a role in the regulation of agonist selection. Despite these observations, the mechanism(s) by which PD-1 contributes to agonist selection remains unclear.

In this study, we define the expression of PD-1 and its ligands, PD-L1 and PD-L2, during thymocyte development. We demonstrate that PD-1 specifically restrains thymically derived Tregs because other populations of alternative lineages that undergo agonist selection, such as NKT cells, remain unchanged. Interestingly, PD-1$^{-/-}$ thymocytes produce more IL-2, a Treg niche–limiting cytokine, which could be responsible for the increase selection of Tregs in PD-1–deficient animals. Our findings highlight the importance of understanding the role of PD-1 in regulating T cell development with implications for the blockade of this pathway in the context of cancer and infections.

MATERIALS AND METHODS

Animals

C57BL/6 (stock no. 000664), C57BL/6;CD90.1 (also referred to as Thy1.1, stock no. 000406), and C57BL/6;CD45.1 (also referred to as B6.SJL, stock no. 002014) mice were purchased from The Jackson Laboratory. PD-L1$^{-/-}$ mice and PD-1$^{-/-}$ mice were a gift from A.H. Sharpe (Harvard Medical School, Boston, MA). Nur77-GFP mice were previously described (19) and purchased from The Jackson Laboratory. All animals were maintained under specific pathogen-free conditions in the Oregon Health & Science University (Portland, OR) animal facility.

Thymic epithelial cell, thymocyte, and lymphocyte isolation

TECs were isolated and enriched as previously described (20). For thymocyte isolation, thymi were harvested and disrupted with a 1-ml syringe plunger through a 70-μm nylon cell strainer (BD Biosciences) and filtered to obtain a single-cell suspension using PBS containing 2% FBS and 0.01% sodium azide. Spleens were harvested and processed to obtain single-cell suspensions using the frosted ends of microscope slides in PBS containing 2% FBS and 0.01% sodium azide. Spleens were incubated with ammonium chloride potassium lysing buffer (Lonza) for 3 min at room temperature to lyse RBCs. Cells were rinsed with PBS containing 2% FBS and 0.01% sodium azide.

Flow cytometry

For flow cytometric analysis, thymocytes and splenocytes were incubated for 20 min at 4°C with LIVE/DEAD Fixable Aqua (Thermo Fisher) and mouse BD Fc block (BD Pharmingen) in PBS. When indicated, cells were incubated for 20 min at room temperature with PBS-57–loaded CD1d tetramer (NIH tetramer core). Cells were then incubated for 20 min at 4°C with the following extracellular Abs: CD5 (53-7.3), CD44 (IM7), TCRβ (H57-597), CD8b (H35-17.2), PD1 (J43), CD8a (53-6.7), CD4 (RM4-5 or GK1.5), CD24 (M1/69), CD25 (PC61.5), CD28 (37.51), CD45.1 (A20), CD69 (H1.2F3), CD73 (TY/11.8), PD-L1 (10F.9G2), PD-L2 (TY25), Thy1.2 (53-2.1), Thy1.1 (HIS51), and Qa2 (695H1-9-9). TECs were incubated for 20 min at 4°C with LIVE/DEAD Fixable Aqua (Thermo Fisher) and the following extracellular Abs: UEA1 (biotin), Ly-51 (6C3), CD45 (30-F11), MHCII (M5/114.15.2), Epcam (G8.8), PD-L1 (10F.9G2), and PD-L2 (TY25). Intracellular protein Foxp3 (FJK-16 s) and Ki67 (SolA15) were detected using the Foxp3 Transcription Factor Concentrate and Diluent (eBioscience). Intracellular protein IL-2 (JES6-5H4) was detected with the BD Fixation/Permeabilization kit (BD Biosciences). All Abs and viability dyes were purchased from BioLegend, BD Biosciences, eBioscience, or Invitrogen. Data were collected with a Fortessa flow cytometer (BD Biosciences) and analyzed using FlowJo software (FlowJo LLC).

BrdU labeling

Animals were injected with 200 μg BrdU (Sigma-Aldrich) i.p. After 24 h, thymi were harvested and processed to a single-cell suspension as described. For detection of BrdU incorporation,

thymocytes were fixed with BD Fixation/Permeabilization buffer (BD Biosciences) for 20 min at room temperature followed by incubation with BD Cytoperm Permeabilization Buffer Plus (BD Biosciences) for 10 min on ice. Cells were then refixed with BD Fixation/Permeabilization buffer (BD Biosciences) for 5 min at room temperature. Thymocytes were treated with 30 μg DNase I for 1.5 h at 37°C to expose BrdU epitopes. Flow cytometric staining was then performed with BrdU (Bu20a).

Bone marrow chimera generation

Femur and tibia bones were harvested from animals, and a 27-gauge needle was used to flush out the bone marrow. The bone marrow was filtered through a 70-μm nylon cell strainer (BD Biosciences) using a 1-ml syringe plunger and rinsed with PBS containing 2% FBS. Mature $CD8^+$ T cells were depleted using CD8a-PE (53-6.7) and the EasySep PE-positive selection kit (STEMCELL Technologies). Animals received a 500-rad X-ray followed by a 450-rad X-ray 4 h later to lethally irradiate the animals in an CIX2 X-Ray Cabinet (Xstrahl). Mice were then anesthetized using isoflurane and reconstituted with 1×10^6–5×10^6 cells injected retroorbitally. Animals were maintained on antibiotic drinking water with 2 mg/ml of neomycin sulfate (Life Technologies) for 2 wk.

In vitro activation and intracellular cytokine staining

Thymocytes were plated at 1×10^6 cells/well in 96-well plates and stimulated for 8 h with PMA (80 nM) and ionomycin (1.3 μM) in the presence of brefeldin A. Cells were then stained for surface markers, fixed and permeabilized using the BD Fixation/Permeabilization kit (BD Biosciences), and stained for intracellular cytokines.

Phospho-STAT5 identification by flow cytometry

Thymocytes were stained with LIVE/DEAD Fixable Aqua (Thermo Fisher) at 4°C for 20 min. Cells were then rested in prewarmed serum-free RPMI for 30 min at 37°C to allow dephosphorylation of STAT5 from in vivo signaling. Cells were stimulated with prewarmed IL-2 in RPMI (1 ng/ml, 0.25 ng/ml, 0.05 ng/ml, 0 ng/ml) for 30 min in a 37°C water bath. At the end of the incubation, cells were immediately placed on ice, and ice-cold fixative from the Foxp3 Transcription Factor Concentrate and Diluent kit (eBioscience) was added. Cells were allowed to fix and permeabilize for 20 min on ice. Cells were then stained for Foxp3 and refixed with 4% paraformaldehyde on ice for 30 min followed by repermeabilization with prechilled 90% methanol. Then, the samples were stained with pSTAT5 (pY694) (BD Biosciences) or isotype control at room temperature for 40 min followed by cell surface markers at room temperature for 20 min.

Phospho-AKT identification by flow cytometry

Thymocytes were rested at 37°C for 20 min to allow for dephosphorylation of AKT. Cells were then stained with LIVE/DEAD Fixable Aqua (Thermo Fisher) at 4°C for 20 min. Cells were washed and incubated with 5 μg/ml anti-CD3-biotin (Invitrogen) and 5 μg/ml anti-CD28-biotin (BD Biosciences) along with extracellular markers on ice for 15 min. To stimulate the cells, the cells were incubated with 20 μg/ml of streptavidin (Thermo Fisher) for the indicated time points (0, 2, 5, or 10 min) at 37°C before being fixed with Phosflow Lyse/Fix Buffer (BD Biosciences) for 10 min at 37°C. Cells were washed and resuspended with prechilled Phosflow Perm Buffer III (BD Biosciences) dropwise and incubated on ice for 1 h. Cells were washed twice before being stained with either isotype control (Cell Signaling Technology) or pAKT (pS473) (Cell Signaling Technology) overnight at 4°C.

Cell sorting for single-cell RNA sequencing (scRNAseq)

Thymi from four wild-type (WT) or PD-$1^{-/-}$ mice were pooled. Thymocytes were obtained as previously described. $CD8a^+$ cells were depleted using CD8a-biotin (53-6.7) and rapid spheres (STEMCELL Technologies). This was followed by another depletion of $CD8b^+$ cells using CD8b-biotin (H35-17.2) to adequately enrich for $CD4^+$ thymocytes. Cells were stained with LIVE/DEAD Fixable Aqua (Thermo Fisher) followed by extracellular staining for CD24 (M1/69), CD25 (PC61.5), CD73 (TY/11.8), CD4 (RM4-5), and CD8a (53-6.7). $CD25^-$ and $CD25^+$ populations were then sorted (Supplemental Fig. 3A). Cell sorts were performed on an Aria (BD Biosciences) with an 85-μm nozzle.

Sample sequencing and alignment

Sorted cells underwent scRNAseq library preparation using the 10X Genomics Chromium platform. Single-cell capturing and cDNA library generation were performed using the Next GEM Single Cell 5′ Reagent Kit version 2 (10X Genomics) according to the manufacturer's instructions. Sequencing was performed following 10X Genomics instructions using the NovaSeq 6000 (Illumina) at the Massively Parallel Sequencing Shared Resource at Oregon Health & Science University. Raw sequencing reads were aligned to the mouse reference genome GRCm38 and quantified using CellRanger (10X Genomics, version 6.2.1). The sequencing data generated in this study are available in the Gene Expression Omnibus database under accession number GSE255727 (https://www.ncbi.nlm.nih.gov/geo/query/acc.cgi?acc=GSE255727).

Single-cell processing and normalization

Unless otherwise specified, all single-cell analysis was performed using R version 4.2.2 and Seurat version 4.3.0 (21). All Seurat objects were merged, and cells were filtered to include only those with greater than 500 features and less than 25% of reads aligning to mitochondrial genes. Cell cycle scoring was performed for each cell by taking mouse analogs of the provided S and G_2M gene lists from Seurat as input into the CellCycleScoring function. Read counts were normalized using the NormalizeData and ScaleData wrappers from Seurat with S and G_2M scores regressed. The FindVariableFeatures

https://doi.org/10.4049/immunohorizons.2300079

function was used to identify the 2000 most variable genes for downstream analysis.

Single-cell clustering

Principal component analysis was performed using the 2000 most variable features, and the first 10 components were determined to capture the most dataset variance, based on the elbow plot. Clustering was then performed after calculating nearest neighbors using the 10 selected principal components as input to the FindNeighbors function. Clustering was performed using the Louvain algorithm with a clustering resolution of 0.5. This resolution was selected by minimizing the average silhouette width per cluster across all clusters identified using the FindClusters function with resolutions ranging from 0.2 to 0.7. Cluster stability across neighboring resolutions was visually assessed using the clustree package (22) (Supplemental Fig. 3B). Positive differentially expressed markers for each of the 14 identified clusters were determined using Seurat's FindAllMarkers function, and manual cell type annotation was performed on the basis of the top markers for each cluster as well as canonical markers defined in literature (Fig. 5B, 5C).

Gene set enrichment

Gene set enrichment analysis (GSEA) was performed to broadly compare WT versus PD-1$^{-/-}$ enrichment, as well as to independently compare enrichment in WT versus PD-1$^{-/-}$ semimature Tregs specifically (cluster 0 versus cluster 1). In each instance, differentially expressed genes (DEGs) between the two groups were identified using the Seurat FindMarkers function with a minimum $\log_2$ fold threshold of 0.2. DEG lists were ordered by $\log_2$ fold change, and GSEA was performed using the msigdb R package from the Molecular Signatures Database (23). When identifying enriched gene sets, all Hallmark gene sets were considered, as well as 16 immune specific gene sets from the Reactome database.

Statistical analysis

Statistical analysis was performed using either an unpaired two-tailed Student *t* test or multiple unpaired *t* tests using the Holm-Šídák method of correction for multiple comparisons in GraphPad Prism 9 (GraphPad Software). Data are presented as mean values with error bars representing SEM. Statistical tests and *p* values are specified for each panel in the respective figure legends, and *p* values <0.05 were considered significant. Biological replicates (individual animals) for each experiment are indicated in the figure legends. All experiments were repeated as indicated in the figure legends.

Study approval

All animal experiments were approved by the institutional animal care and use committee of Oregon Health & Science University (Portland, OR).

RESULTS

PD-1 and its ligands, PD-L1 and PD-L2, are expressed in the thymus

It has previously been established that PD-1 and its ligands are expressed in the thymus (11, 12), but the kinetics of PD-1 expression throughout thymocyte development remain undefined. To determine thymic expression of PD-L1 and PD-L2, thymi from 6-wk-old mice were harvested and enriched for TECs to examine the expression of PD-L1 and PD-L2 in cortical (UEA1^{lo} Ly51^{hi}) and medullary (UEA1^{hi}, Ly51^{lo}) TECs using flow cytometry. PD-L1 was expressed equally on both cortical TECs (cTEC) and medullary TECs (mTECs), whereas PD-L2 was expressed only in a subset of mTECs (Fig. 1A, 1B). Next, we examined PD-1 expression across thymocyte development (Supplemental Fig. 1A) and found that a subset of DN1 and DN4 highly expressed PD-1 (Fig. 1C, 1D, Supplemental Fig. 1A). In postpositive selection thymocyte subsets, we observed NK T (NKT) cells were the highest expressers of PD-1 (Fig. 1C, 1D, Supplemental Fig. 1A). Interestingly, we found that thymocytes also expressed PD-L1, with agonist selected cell populations such as Tregs and NKT cells (Fig. 1E, 1F) having some of the highest expression. Notably, thymocytes did not express much PD-L2, especially compared with PD-L1 (Supplemental Fig. 1B, 1C). These data demonstrate that PD-1 and its ligands are expressed throughout thymocyte development and could play a role in regulating the development of T cells.

PD-1 restrains thymic Treg development

Given that PD-1 and its ligands are expressed in the thymus, PD-1 signaling could regulate thymocyte maturation. Indeed, previous studies have suggested that PD-1 inhibits β selection (15, 16), but PD-1's role in regulating other stages of thymocyte development has not been well characterized. To elucidate the role of PD-1 in thymocyte development, we examined the thymus of 3-wk-old PD-1$^{-/-}$ animals. We found that there were no differences in the early double-negative (DN1–4) stages of thymocyte development (Fig. 2A–C) in PD-1–deficient animals. In contrast, PD-1$^{-/-}$ animals had a significant increase in Tregs (CD4$^+$CD25$^+$Foxp3$^+$), along with CD25$^+$ TregP (CD4$^+$CD25$^+$) and Foxp3$^+$ TregP (CD4$^+$Foxp3$^+$) Treg progenitors (Fig. 2D–F). However, not all agonist selected T cell populations were expanded because NKT cell frequencies remained unchanged (Fig. 2E). To ensure that these Tregs were not recirculating, we used the marker CD73, which has been reported to distinguish newly developing cells in the thymus (CD73$^-$) from recirculating cells from the periphery (CD73$^+$) (24, 25). We therefore examined CD73$^-$ cells and quantified Tregs and their progenitors. We found that the significant increase in Tregs remained when CD73$^-$ cells were examined (Supplemental Fig. 1D, 1E).

We next explored whether PD-1 limits Treg development in a cell-intrinsic manner. To answer this question, mixed bone marrow chimeras were generated at a ratio of 1:1 (WT:PD-1$^{-/-}$ or WT:WT) (Supplemental Fig. 1G). Consistent with our

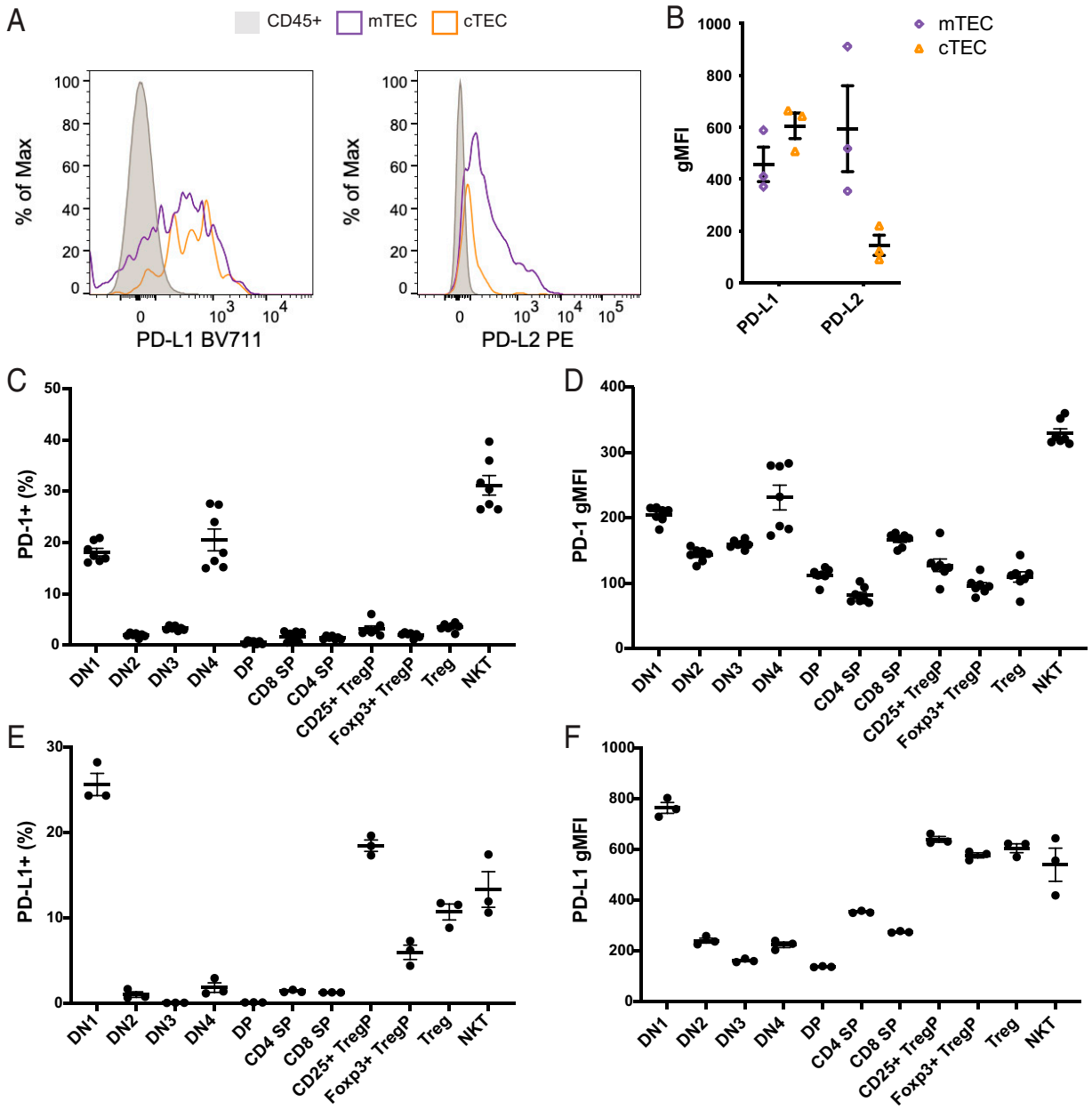

FIGURE 1. PD-1 and its ligands, PD-L1 and PD-L2, are expressed in the thymus.

(**A**) Thymi were harvested from 6-wk-old WT mice (n = 3) and depleted of $CD45^+$ thymocytes by panning to enrich for TECs. Staining for PD-L1 and PD-L2 in mTECs and cTECs and (**B**) gMFI of PD-L1 and PD-L2 in mTECs and cTECs. Data are representative of three independent experiments. (**C**) Thymi were harvested from 3-wk-old WT mice. Frequency of $PD\text{-}1^+$ cells and (**D**) gMFI of PD-1 from two combined experiments (n = 7). (**E**) Frequency of PD-L1 and (**F**) gMFI of PD-L1 across thymocyte development (n = 3). Data are representative of three independent experiments.

observations in $PD\text{-}1^{-/-}$ mice, there was a significant increase in Tregs in the $PD\text{-}1^{-/-}$ donor T cells compared with WT cells. Notably, we also observed an increase in Tregs in WT donor T cells in the WT:$PD\text{-}1^{-/-}$ mixed bone marrow chimeras compared with controls (Fig. 2G).

To understand the contribution of PD-L1 in supporting the phenotype we observed, we examined $PD\text{-}L1^{-/-}$ animals and also observed an increase in Tregs but not NKT cells (Supplemental Fig. 1F), further suggesting that PD-1 signaling is specifically regulating Treg development. Because some thymocyte populations expressed high levels of PD-L1, we speculated that PD-L1 on the stromal cells could be contributing to Treg development. Thus, we generated bone marrow chimeras of WT bone marrow into either WT or $PD\text{-}L1^{-/-}$ mice. We observed an increase in Tregs specifically in the $PD\text{-}L1^{-/-}$ animals (Fig. 2H), suggesting that PD-L1 on the stromal cells contributes to Treg development.

https://doi.org/10.4049/immunohorizons.2300079

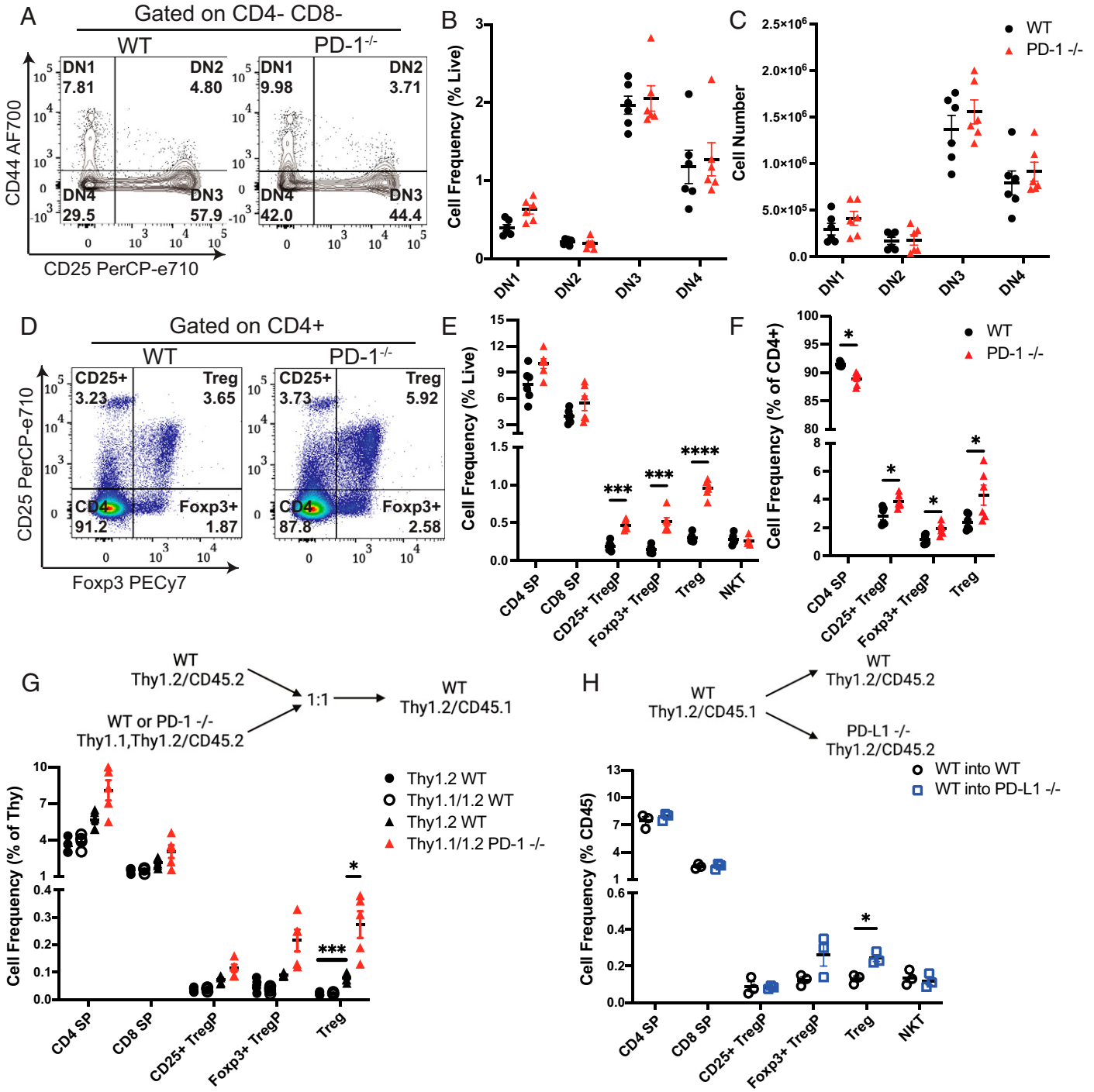

FIGURE 2. PD-1 signaling restrains thymic Treg development.

Thymi were harvested from 3-wk-old WT or PD-1$^{-/-}$ mice (n = 6). (**A**) Identification of DN thymocyte populations and quantification of DN populations as (**B**) percentage live and (**C**) cell number. (**D**) Identification of Tregs and their progenitor populations using expression of CD25 and Foxp3 to delineate CD4 SP (CD25$^-$ Foxp3$^-$), CD25$^+$ TregP (CD25$^+$ Foxp3$^-$), Foxp3$^+$ TregP (CD25$^-$ Foxp3$^+$), and Treg (CD25$^+$ Foxp3$^+$) and quantification of thymocyte populations as (**E**) percentage live and (**F**) cell number. Data are combined from two experiments. (**G**) Schematic demonstrating the generation of mixed bone marrow chimeras. Thymi were harvested 6 wk after reconstitution (n = 5). The frequency of thymocyte populations is presented as percentage congenic marker (Thy). Data are representative of two independent experiments. (**H**) Schematic demonstrating the generation of bone marrow chimeras. Thymi were harvested 6 wk after reconstitution (n = 3). The frequency of thymocyte populations is presented as percentage congenic marker (CD45). Data are representative of three independent experiments. Multiple unpaired t tests using the Holm-Šídák correction for multiple comparisons. *$p < 0.05$, ***$p < 0.001$, ****$p < 0.0001$.

https://doi.org/10.4049/immunohorizons.2300079

PD-1–deficient thymocytes are more mature

Given the increase in Tregs in PD-1$^{-/-}$ thymi, we postulated that perhaps in the absence of this coinhibitory signal, thymocytes are pushed through maturation at an accelerated rate. To explore this, thymi from 5-wk-old WT and PD-1$^{-/-}$ animals were profiled with markers that distinguish immature from mature thymocytes, HSA (also known as CD24), and Qa2 (26, 27). Developing thymocytes downregulate HSA and upregulate Qa2 as they mature, allowing for identification of immature and mature thymocyte using these markers. Interestingly, there were fewer immature thymocytes (HSA^{hi}Qa2^{lo}) and more mature (HSA^{lo}Qa2^{hi}) CD4 SP and CD25^{+} TregP thymocytes in PD-1$^{-/-}$ animals (Fig. 3A, 3B).

Because these thymocytes appear to be more mature, we hypothesized that the PD-1–deficient cells may be more proliferative, leading to an increase in Tregs. Importantly, we saw no difference in cell proliferation as measured by Ki67 (Fig. 3C, Supplemental Fig. 2A). We also evaluated proliferation by injecting 3-wk-old WT and PD-1$^{-/-}$ animals with 200 μg BrdU i.p. and harvested thymi 24 h later. We saw no difference in the frequency of BrdU^{+} cells between WT and PD-1$^{-/-}$ animals (Fig. 3D, Supplemental Fig. 2A). Taken together, these data suggest that the increased abundance of Tregs is not due to a proliferative advantage.

An alternative hypothesis for the increase in Tregs is that the death of these cells is compromised in PD-1$^{-/-}$ animals.

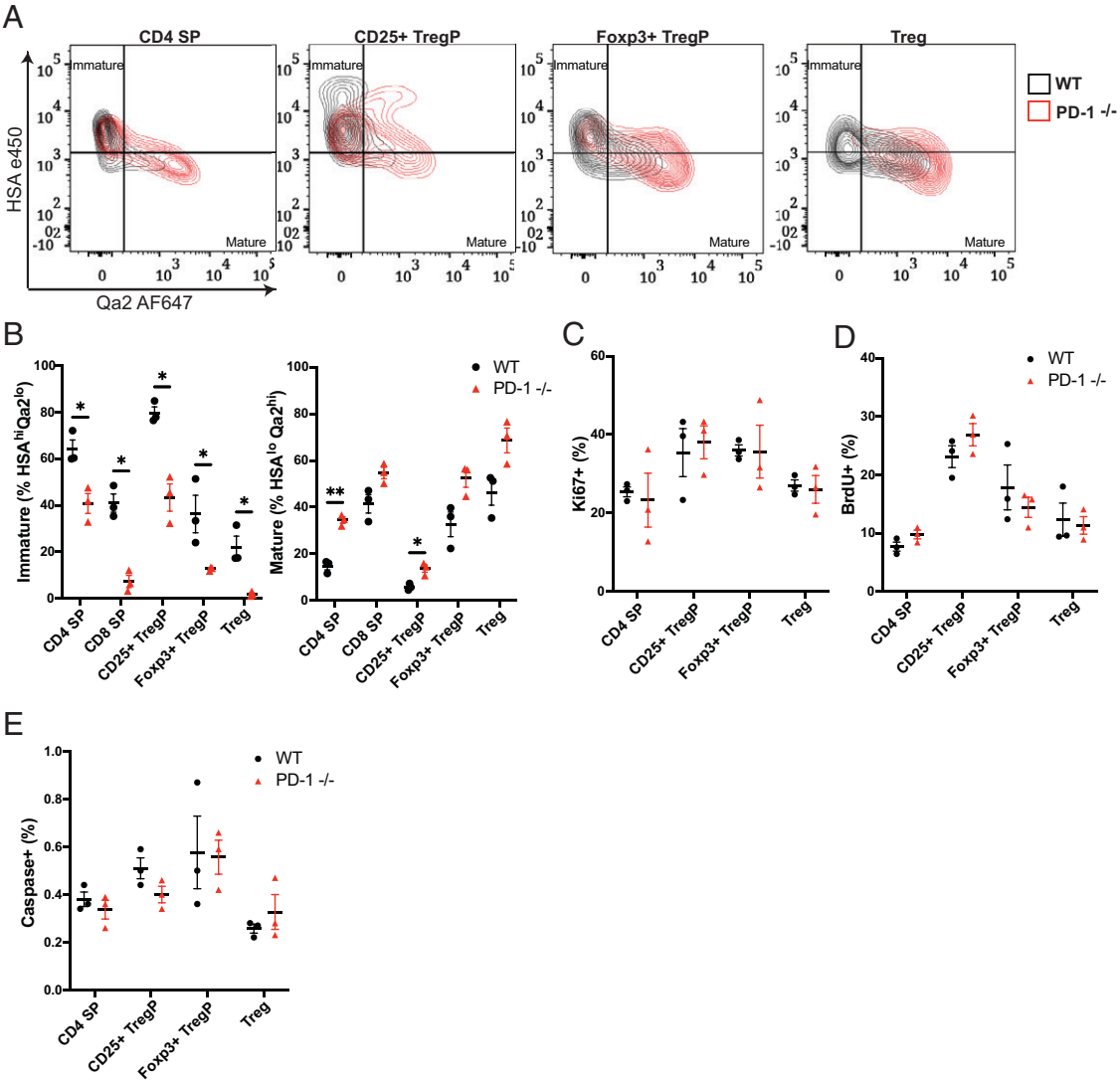

FIGURE 3. PD-1 deficiency leads to an increase in thymocyte maturation with no difference in cell proliferation or cell death.

Thymi were harvested from 5-wk-old WT or PD-1$^{-/-}$ mice (n = 3). (**A**) Flow plots for the expression of HSA and Qa2. (**B**) Quantification of immature cells (%HSA^{hi}Qa2^{lo}) and mature cells (%HSA^{lo}Qa2^{hi}). (**C**) 3-wk-old WT or PD-1$^{-/-}$ mice (n = 3) were injected with 200 μg BrdU i.p. Thymi were harvested 24 h later and stained for proliferation markers and cleaved caspase-3 to mark dying cells. Quantification of Ki67^{+} cells (%). (**D**) Quantification of BrdU^{+} cells (%). (**E**) Quantification of cleaved caspase-3^{+} cells (%). Data are representative of three independent experiments. Multiple unpaired t tests using the Holm-Šídák correction for multiple comparisons. *$p < 0.05$.

https://doi.org/10.4049/immunohorizons.2300079

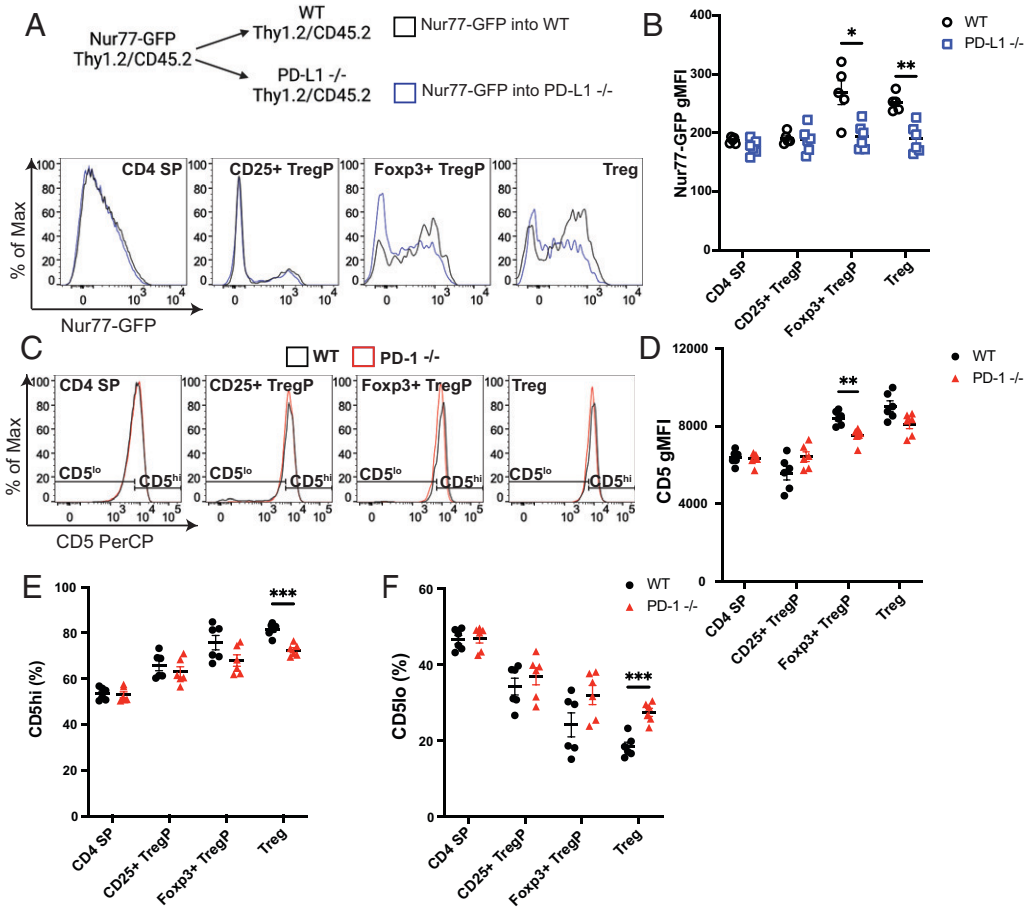

FIGURE 4. PD-1 deficiency alters TCR signal strength.

(**A**) Schematic of bone marrow chimera generation. Thymi were harvested after 6 wk of reconstitution ($n = 5$). Histograms depicting Nur77-GFP expression and (**B**) gMFI of Nur77-GFP. Data are representative of two independent experiments. (**C**) Thymi were harvested from 3-wk-old WT or PD-$1^{-/-}$ mice ($n = 6$). Histograms depicting CD5 expression. CD4 SP thymocytes were gated so that the top 50% of cells were $CD5^{hi}$ and the bottom 50% of cells were $CD5^{lo}$, and then gates were applied to all populations of interest. Representative of three independent experiments. (**D**) CD5 gMFI and (**E**) frequency of $CD5^{hi}$ and (**F**) $CD5^{lo}$ cells. Data are combined from two independent experiments. Multiple unpaired *t* tests using the Holm-Šídák correction for multiple comparisons. $*p < 0.05$, $**p < 0.01$, $***p < 0.001$.

We examined cell death through staining thymocytes from 3-wk-old WT and PD-$1^{-/-}$ animals for cleaved caspase-3. We observed no differences in cleaved caspase-3 staining in WT and PD-$1^{-/-}$ animals (Fig. 3E, Supplemental Fig. 2B), suggesting that the increase in Tregs in PD-1–deficient thymocytes was not due to diminished cell death.

PD-1 deficiency alters TCR signal strength

Given that PD-1 can temper TCR signaling (7), we sought to determine whether PD-1 was restraining Treg development through modulation of TCR signaling. It has been demonstrated that Nur77 expression correlates with TCR signal strength such that higher levels of Nur77 indicate stronger signaling through the TCR (19). To assess Nur77 expression when PD-1 signaling is disrupted, we reconstituted WT or PD-$L1^{-/-}$ mice with bone marrow from Nur77-GFP reporter animals. We evaluated thymi 6–8 wk after reconstitution and noted a decrease in Nur77-GFP expression in $Foxp3^{+}$ TregP and Tregs in PD-$L1^{-/-}$ recipient mice (Fig. 4A, 4B) compared with WT. When we specifically looked at Nur77-GFP^{+} cells and examined the geometric mean fluorescence intensity (gMFI) of the GFP^{+} cells, we found a significant decrease in overall Nur77-GFP expression in CD4 SP, $CD25^{+}$ TregP, $Foxp3^{+}$ TregP, and Treg in the PD-$L1^{-/-}$ compared with WT mice (Supplemental Fig. 2C).

Because Nur77 expression was decreased when PD-1 signaling was disrupted, we hypothesized that thymocytes with lower-affinity TCRs were being selected into the Treg lineage in the absence of PD-1. To test this hypothesis, we examined expression of CD5, which is known to correlate with TCR signal strength (28–30). We determined that overall CD5 expression was reduced on $Foxp3^{+}$ TregP (Fig. 4C, 4D). Because changes in CD5 expression are often subtle, we gated the top 50% of CD5-expressing cells as $CD5^{hi}$ and the bottom 50% as $CD5^{lo}$ based on the CD4 SP population and applied these

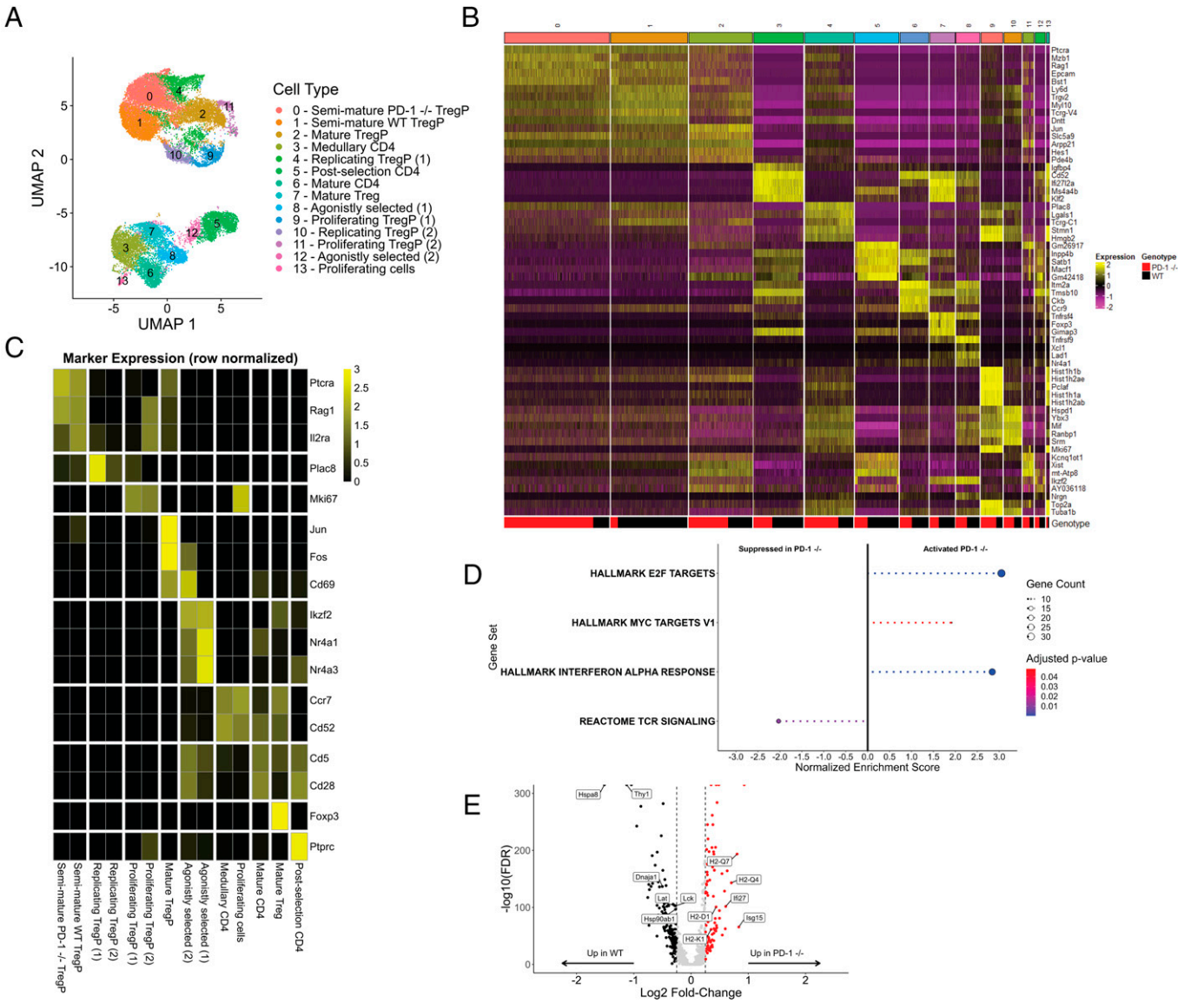

FIGURE 5. PD-1–deficient cells are more mature despite lower TCR signaling.

Thymi were harvested from 3-wk-old WT or PD-$1^{-/-}$ mice (n = 3) and pooled for FACS. $CD4^+CD25^-$ (CD4) and $CD4^+CD25^+$ (Treg+P) populations were sorted, and scRNAseq was performed using the 10X Genomics platform. (**A**) Uniform Manifold Approximation and Projection (UMAP) of all cells that passed quality control (24,655 cells). (**B**) Heatmap showing scaled expression of top markers ranked by fold change in each cluster. (**C**) Heatmap showing top markers used to call clusters. (**D**) Activated and suppressed hallmark pathways in PD-$1^{-/-}$ compared with WT in pseudo-bulk analysis. (**E**) Volcano plot of DEGs in cluster 0 (semimature PD-$1^{-/-}$ TregP) versus cluster 1 (semimature WT TregP).

gates to all populations of interest (Fig. 4C). Using this gating strategy, we found that there was a decrease in the $CD5^{hi}$ Treg population in PD-$1^{-/-}$ cells compared with WT (Fig. 4E) with a concomitant increase in the $CD5^{lo}$ Treg population (Fig. 4F). CD5 levels are thought to be set in the thymus and then persist in the periphery, so we examined CD5 expression in splenocytes and found a decrease in Treg CD5 gMFI (Supplemental Fig. 2D). These data suggested that PD-1 may limit Treg development by regulating TCR signal strength.

scRNAseq confirms a decrease in TCR signal strength and an increase in maturity markers in PD-$1^{-/-}$ thymocytes

To understand how PD-1 is regulating Treg development, we sorted $CD4^+CD25^-$ thymocytes, which contain conventionally selected CD4s (termed CD4), and $CD4^+CD25^+$, which contain Tregs and the $CD25^+$ TregP (termed Treg+P), from 3-wk-old WT and PD-$1^{-/-}$ thymi (Supplemental Fig. 3A). Because there are relatively limited numbers of Tregs and their progenitors in the thymus, we performed scRNAseq using the 10X Genomics platform. We captured 28,302 cells in total, and

https://doi.org/10.4049/immunohorizons.2300079

24,655 cells passed quality control and were taken on for further analysis. Fourteen unique clusters were identified (Fig. 5A–5C, Supplemental Fig. 3B), with one large cluster comprising mostly TregP and a second comprising CD4 and Treg (Supplemental Fig. 3C). To begin understanding differences between cells sorted from WT or PD-1$^{-/-}$ animals, we performed a pseudo-bulk analysis comparing WT with PD-1$^{-/-}$ cells followed by GSEA. This analysis suggested that TCR signaling was significantly downregulated in PD-1$^{-/-}$ cells compared with WT cells, whereas MYC targets and E2F targets were significantly upregulated in PD-1$^{-/-}$ (Fig. 5D). Indeed, we found that *Cd5* gene expression was down in PD-1$^{-/-}$ cells from our scRNAseq analysis (Supplemental Fig. 3D, $p < 1 \times 10^{-16}$), corroborating the findings of our protein analysis.

Upon further analysis of our scRNAseq data, we noted that cluster 0 and cluster 1 were the only clusters to separate primarily on the basis of mouse genotype, representing TregP cells from PD-1$^{-/-}$ and WT, respectively (Fig. 5B, Supplemental Fig. 3C). By performing differential gene expression analysis, we identified Thy1 as one of the genes most differentially expressed between PD-1$^{-/-}$ and WT TregP cells (Fig. 5E). PD-1$^{-/-}$ cells were congenically marked with Thy1.1 and lack WT Thy1.2 expression, reiterating the strong separation of PD-1$^{-/-}$ and WT cells between clusters 0 and 1, respectively. In addition, genes downstream of TCR/CD28 signaling (Lat and Lck), as well as heat shock genes (Hspa8, Hsp90aa1, Dnaja1), were significantly downregulated in PD-1$^{-/-}$ thymocytes. Interestingly, a recent study has demonstrated that signaling through LAT specifically regulates T cell development through its regulation of negative selection and promotion of Treg development (31). Genes with greater expression in PD-1$^{-/-}$ thymocytes included those associated with IFN signaling (Ifi27, Isg15) and histocompatibility genes (H2-Q7, H2-Q4, H2-K1, H2-D1). Importantly, H2-Q7 encodes the protein Qa2, which we identified was upregulated in PD-1–deficient thymocytes because these thymocytes were more mature (Fig. 3A, 3B). We also performed GSEA on the DEGs identified and found that IFN responses were activated, whereas TNF signaling was suppressed, in PD-1$^{-/-}$ cells (Supplemental Fig. 3E).

PD-1$^{-/-}$ thymocytes have subtle increases in CD28 expression

PD-1 directly inhibits CD28 signaling, which is critical for Treg development (8, 32). Therefore, we determined if there were any changes in CD28 expression in PD-1–deficient cells and found that there was a subtle increase in CD28 expression in Foxp3^{+} TregP and Treg in PD-1$^{-/-}$ animals (Fig. 6A, 6B). We also examined CD28 expression in PD-L1$^{-/-}$ animals and saw an increase in CD4 SP, CD25^{+} TregP, Foxp3^{+} TregP, and Tregs (Supplemental Fig. 4A, 4B).

PD-1–deficient T cells produce more IL-2

It has been reported that signaling through CD28 induces IL-2 production (33, 34). In light of the observation that WT thymocytes in the presence of PD-1–deficient thymocytes have an increased frequency of Tregs (Fig. 2G) and that IL-2 is a Treg niche limiting cytokine in the thymus (35–38), we speculated that perhaps PD-1 was regulating thymic IL-2 levels. We examined IL-2 production in bulk thymocytes stimulated with PMA and ionomycin for 8 h and observed a 2-fold increase in IL-2^{+} PD-1$^{-/-}$ thymocytes (Fig. 6C, 6D). Similar results were obtained when bulk thymocytes were stimulated with anti-CD3/CD28 (Supplemental Fig. 4C). It has previously been reported that other CD4 SP thymocytes produce the majority of IL-2 in the thymus (39). To determine the dominant source of IL-2 in PD-1$^{-/-}$ thymocytes, we examined all IL-2^{+} cells for CD4 or CD8 expression. Surprisingly, we found that the increase in IL-2^{+} production was driven largely by CD8^{+} cells in PD-1$^{-/-}$ animals (Fig. 6E). This observation is intriguing, given that CD8 SP thymocytes express about twice as much PD-1 as CD4 SP (Fig. 1D). To confirm that the PD-1–deficient cells were producing more IL-2, we harvested the cell supernatants and measured IL-2 concentration by ELISA and found that there was significantly more IL-2 present in the supernatants of PD-1$^{-/-}$ cell cultures (Fig. 6F).

The increase in IL-2 availability could drive an increase in Treg selection. Thus, we sought to determine if PD-1$^{-/-}$ thymocytes were more sensitive to IL-2 signaling. We measured STAT5 phosphorylation in WT and PD-1–deficient thymocytes stimulated with increasing concentrations of IL-2. We found no difference in the frequency of pSTAT5^{+} cells or pSTAT5 gMFI in WT compared with PD-1$^{-/-}$ thymocytes (Supplemental Fig. 4D, 4E), suggesting that there is no difference in sensitivity to IL-2 in PD-1–deficient animals; rather, there is a global increase in the availability of this cytokine in the thymus.

DISCUSSION

The emergence of PD-1 targeted therapies as standard of care treatment for many patients with cancer has changed the clinical landscape of oncology. Over the past 10 years, thousands of studies have sought to understand the mechanisms of anti-PD-1 response and resistance. Several studies in the periphery have highlighted the importance in PD-1 for restraining T cell proliferation. However, very few studies have explored the importance of PD-1 during T cell development and differentiation. We propose that by studying a developmental role of PD-1 in the thymus, we might understand the biology of PD-1 blockade in the periphery. In this study, we demonstrate that PD-1 is expressed early on the cell surface of developing thymocytes at the DN stage. These data agree with previous reports that describe PD-1 expression in DN thymocytes (11, 15). We further elucidate the expression of PD-L1 and PD-L2, finding that PD-L1 is expressed in cTECs and mTECs, whereas PD-L2 expression is restricted to mTECs. Using immunohistochemistry, others have reported PD-L1 expression distributed throughout the thymus, whereas PD-L2 expression is restricted to the medulla, in agreement with our findings (12, 40). In our study, we did not examine other thymic APCs, such as dendritic cells,

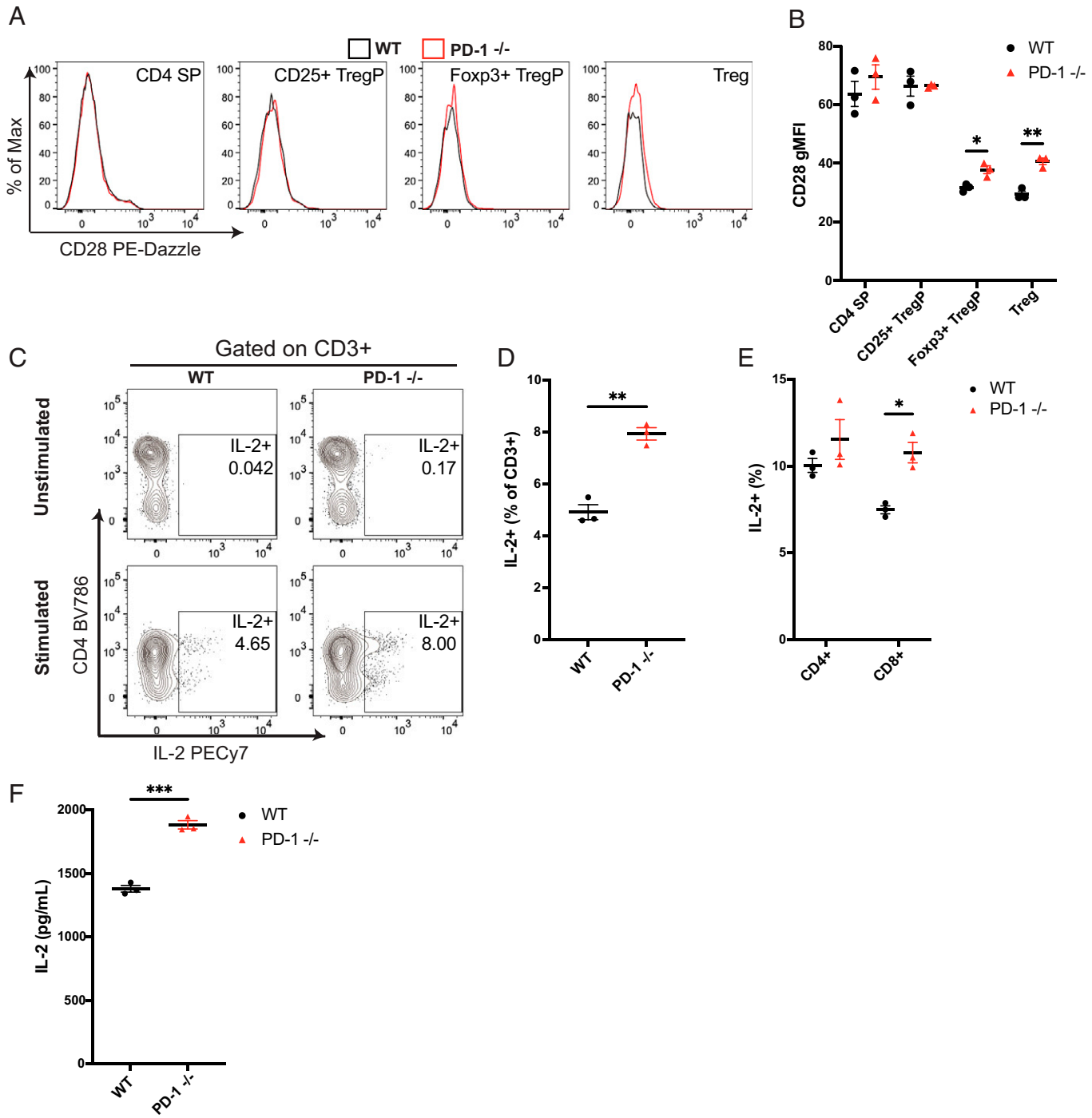

FIGURE 6. PD-1–deficient cells produce more IL-2 despite no change in response to CD28 signaling.

(**A**) Thymi were harvested from 3-wk-old WT or PD-$1^{-/-}$ mice ($n = 3$). Histograms depicting CD28 expression and (**B**) quantification of CD28 gMFI. Data are representative of two independent experiments. (**C**) Bulk thymocytes were harvested from 3-wk-old WT or PD-$1^{-/-}$ mice ($n = 3$) and stimulated with PMA/ionomycin for 8 h. Flow plots depicting gating of IL-2^+ cells in unstimulated and stimulated cells from WT or PD-$1^{-/-}$ animals. (**D**) Frequency of IL-2^+ cells (percentage of $CD3^+$). (**E**) Frequency of $CD4^+$ or $CD8^+$ cells that are IL-2^+. (**F**) Quantification of the amount of IL-2 in the cell supernatants of the cultures by ELISA. Data are representative of three independent experiments. Unpaired Student *t* test or multiple unpaired *t* tests using the Holm-Šídák correction for multiple comparisons. *$p < 0.05$, **$p < 0.01$, ***$p < 0.001$.

which have been reported to express PD-L1 and PD-L2 (40, 41). Interestingly, PD-L1 is known to be expressed by DN and CD8 SP thymocytes, whereas PD-L2 is not expressed on thymocytes at all (42). Our data expand these findings to demonstrate that some of the highest expressers of PD-L1 in the thymus are agonist selected thymocyte populations, including $CD25^+$ TregP,

https://doi.org/10.4049/immunohorizons.2300079

Foxp3$^+$ TregP, Treg, and NKT cells. This led us to ask how PD-1 signaling might impact thymocyte development, especially of agonist selected cell populations.

Several reports have shown that PD-1 regulates peripheral induction of Tregs through its interaction with PD-L1 via the Akt-mTOR pathway (18, 43, 44); however, the role of PD-1 in regulating Treg development in the thymus has not been well studied. There is some evidence that PD-1 limits Treg development: A previous report by Ellestad and colleagues found PD-1$^{-/-}$ hematopoietic stem cells transplanted into Rag2-knockout mice were more likely than WT cells to become Tregs (17). Likewise, Chen and colleagues found an increase in the thymic development of Tregs using both PD-1$^{-/-}$ animals and mixed bone marrow chimeras (18). Interestingly, the authors of both studies determined that PD-1 is not necessary for promoting Treg selection in the thymus but did not follow up on the mechanism by which PD-1 restrains thymic Treg development. Interestingly, our scRNAseq data demonstrate that PD-1$^{-/-}$ and WT Tregs clustered together, indicating that these populations are similar. Additionally, we observed that WT cells in the presence of PD-1–deficient thymocytes were more likely to become Tregs. These data highlight that the impact we observe in PD-1–deficient cells is not cell-intrinsic, but rather a change in the microenvironment. In this study, we demonstrate that PD-1 limits the production of IL-2 within the thymus, thereby restraining the development of Tregs. Despite many indications that IL-2 is critical for Treg development (35–38), at least one recent study indicates that IL-2 is not the obligate cytokine leading to Foxp3 upregulation (45). This study concludes that Foxp3 upregulation requires disruption of agonist signaling by TGF-β under normal physiological conditions, but, in conditions with excessive in vivo IL-2, Foxp3 is upregulated in response to IL-2 signaling. In our model of PD-1–deficient animals, excessive IL-2 may be the driving factor for increased Treg development. One limitation of this study is that PD-1 is absent at all stages of T cell development. More nuanced studies limiting PD-1 deficiency to Treg progenitor populations could further elucidate the mechanism by which PD-1 is restraining Treg development.

Interestingly, we observed that the dominant increase in IL-2 production was from CD8$^+$ thymocytes rather than CD4$^+$ thymocytes. This contrasts with reports which have suggested that CD4$^+$ thymocytes, specifically CD25$^+$ TregP, are the main source of IL-2 in the thymus (24, 38, 39). Other studies have reported that PD-1 limits IL-2 in peripheral CD8$^+$ T cells (46, 47); however, the exact mechanism remains unclear. One attractive hypothesis is that PD-1's inhibition of CD28 signaling leads to a decrease in IL-2 because CD28 signaling is known to facilitate IL-2 production (33, 34). In our study, we see a subtle increase in CD28 present on the cell surface of PD-1$^{-/-}$ Tregs and their Foxp3$^+$ progenitors, as well as in PD-L1$^{-/-}$ Tregs and both progenitor populations. This increase in CD28 expression could translate into the increase in IL-2 production observed. Future studies should seek to elucidate the mechanism by which PD-1 limits IL-2 production in T cells.

We observed a decrease in markers of TCR signal strength, specifically CD5 (28–30) and Nur77 (19), when PD-1 signaling was disrupted in thymocytes, which was corroborated by our sequencing data. These data suggest that the repertoire of Tregs may be different in PD-1$^{-/-}$ animals. One hypothesis that aligns with our findings is that less self-reactive clones are being selected into the Treg repertoire in the absence of PD-1. It would be interesting to explore this hypothesis using PD-1$^{-/-}$ animals on a fixed TCRβ chain background that allow for deep sequencing of the TCRα chains to examine the repertoire.

Most studies of the biology of PD-1 have focused on the role of this pathway in restraining peripheral effector T cell function. Blockade of this inhibitory protein is hypothesized to drive an increase in effector T cells, shifting the effector T cell/Treg ratio to enhance the immune response in tumor and infection models. However, the current findings suggest that blockade of this pathway might yield an increase in thymic Treg populations, which would be undesirable in the context of tumors or infections. By using therapies that systemically target PD-1, we may unknowingly alter the frequency, repertoire, and function of Tregs selected for in the thymus. These alterations could impact response to therapy or the development of adverse events in patients.

DISCLOSURES

The authors have no financial conflicts of interest.

ACKNOWLEDGMENTS

We are grateful to the Oregon Health and Science University (OHSU) Department of Comparative Medicine, the OHSU Flow Cytometry Core, and the OHSU Massively Parallel Sequencing Shared Resource for their outstanding support. We thank Dr. Susan Murray for critical review of the manuscript.

REFERENCES

1. Starr, T. K., S. C. Jameson, and K. A. Hogquist. 2003. Positive and negative selection of T cells. *Annu. Rev. Immunol.* 21: 139–176.
2. Rudd, C. E., A. Taylor, and H. Schneider. 2009. CD28 and CTLA-4 coreceptor expression and signal transduction. *Immunol. Rev.* 229: 12–26.
3. Ishida, Y., Y. Agata, K. Shibahara, and T. Honjo. 1992. Induced expression of PD-1, a novel member of the immunoglobulin gene superfamily, upon programmed cell death. *EMBO J.* 11: 3887–3895.
4. Chemnitz, J. M., R. V. Parry, K. E. Nichols, C. H. June, and J. L. Riley. 2004. SHP-1 and SHP-2 associate with immunoreceptor tyrosine-based switch motif of programmed death 1 upon primary human T cell stimulation, but only receptor ligation prevents T cell activation. *J. Immunol.* 173: 945–954.
5. Dong, H., G. Zhu, K. Tamada, and L. Chen. 1999. B7-H1, a third member of the B7 family, co-stimulates T-cell proliferation and interleukin-10 secretion. *Nat. Med.* 5: 1365–1369.
6. Latchman, Y., C. R. Wood, T. Chernova, D. Chaudhary, M. Borde, I. Chernova, Y. Iwai, A. J. Long, J. A. Brown, R. Nunes, et al. 2001.

PD-L2 is a second ligand for PD-1 and inhibits T cell activation. *Nat. Immunol.* 2: 261–268.
7. Mizuno, R., D. Sugiura, K. Shimizu, T. Maruhashi, M. Watada, I. M. Okazaki, and T. Okazaki. 2019. PD-1 primarily targets TCR signal in the inhibition of functional T cell activation. *Front. Immunol.* 10: 630.
8. Hui, E., J. Cheung, J. Zhu, X. Su, M. J. Taylor, H. A. Wallweber, D. K. Sasmal, J. Huang, J. M. Kim, I. Mellman, and R. D. Vale. 2017. T cell costimulatory receptor CD28 is a primary target for PD-1-mediated inhibition. *Science* 355: 1428–1433.
9. Nishimura, H., M. Nose, H. Hiai, N. Minato, and T. Honjo. 1999. Development of lupus-like autoimmune diseases by disruption of the PD-1 gene encoding an ITIM motif-carrying immunoreceptor. *Immunity* 11: 141–151.
10. Nishimura, H., T. Okazaki, Y. Tanaka, K. Nakatani, M. Hara, A. Matsumori, S. Sasayama, A. Mizoguchi, H. Hiai, N. Minato, and T. Honjo. 2001. Autoimmune dilated cardiomyopathy in PD-1 receptor-deficient mice. *Science* 291: 319–322.
11. Nishimura, H., Y. Agata, A. Kawasaki, M. Sato, S. Imamura, N. Minato, H. Yagita, T. Nakano, and T. Honjo. 1996. Developmentally regulated expression of the PD-1 protein on the surface of double-negative (CD4-CD8-) thymocytes. *Int. Immunol.* 8: 773–780.
12. Liang, S. C., Y. E. Latchman, J. E. Buhlmann, M. F. Tomczak, B. H. Horwitz, G. J. Freeman, and A. H. Sharpe. 2003. Regulation of PD-1, PD-L1, and PD-L2 expression during normal and autoimmune responses. *Eur. J. Immunol.* 33: 2706–2716.
13. Zuklys, S., G. Balciunaite, A. Agarwal, E. Fasler-Kan, E. Palmer, and G. A. Holländer. 2000. Normal thymic architecture and negative selection are associated with Aire expression, the gene defective in the autoimmune-polyendocrinopathy-candidiasis-ectodermal dystrophy (APECED). *J. Immunol.* 165: 1976–1983.
14. Perry, J. S. A., C. J. Lio, A. L. Kau, K. Nutsch, Z. Yang, J. I. Gordon, K. M. Murphy, and C. S. Hsieh. 2014. Distinct contributions of Aire and antigen-presenting-cell subsets to the generation of self-tolerance in the thymus. *Immunity* 41: 414–426.
15. Nishimura, H., T. Honjo, and N. Minato. 2000. Facilitation of beta selection and modification of positive selection in the thymus of PD-1-deficient mice. *J. Exp. Med.* 191: 891–898.
16. Keir, M. E., Y. E. Latchman, G. J. Freeman, and A. H. Sharpe. 2005. Programmed death-1 (PD-1):PD-ligand 1 interactions inhibit TCR-mediated positive selection of thymocytes. *J. Immunol.* 175: 7372–7379.
17. Ellestad, K. K., G. Thangavelu, C. L. Ewen, L. Boon, and C. C. Anderson. 2014. PD-1 is not required for natural or peripherally induced regulatory T cells: severe autoimmunity despite normal production of regulatory T cells. *Eur. J. Immunol.* 44: 3560–3572.
18. Chen, X., D. Fosco, D. E. Kline, L. Meng, S. Nishi, P. A. Savage, and J. Kline. 2014. PD-1 regulates extrathymic regulatory T-cell differentiation. *Eur. J. Immunol.* 44: 2603–2616.
19. Moran, A. E., K. L. Holzapfel, Y. Xing, N. R. Cunningham, J. S. Maltzman, J. Punt, and K. A. Hogquist. 2011. T cell receptor signal strength in Treg and iNKT cell development demonstrated by a novel fluorescent reporter mouse. *J. Exp. Med.* 208: 1279–1289.
20. Xing, Y., and K. A. Hogquist. 2014. Isolation, identification, and purification of murine thymic epithelial cells. *J. Vis. Exp.* (90): e51780.
21. Hao, Y., S. Hao, E. Andersen-Nissen, W. M. Mauck, 3rd, S. Zheng, A. Butler, M. J. Lee, A. J. Wilk, C. Darby, M. Zager, et al. 2021. Integrated analysis of multimodal single-cell data. *Cell* 184: 3573–3587.e29.
22. Zappia, L., and A. Oshlack. 2018. Clustering trees: a visualization for evaluating clusterings at multiple resolutions. *Gigascience* 7: giy083
23. Bhuva, D. S., and A. Garnham. G2023. msigdb: an ExperimentHub package for the Molecular Signatures Database (MSigDB). R package version 1.8.0.
24. Owen, D. L., R. S. La Rue, S. A. Munro, and M. A. Farrar. 2022. Tracking regulatory T cell development in the thymus using single-cell RNA sequencing/TCR sequencing. *J. Immunol.* 209: 1300–1313.
25. Owen, D. L., S. A. Mahmud, L. E. Sjaastad, J. B. Williams, J. A. Spanier, D. R. Simeonov, R. Ruscher, W. Huang, I. Proekt, C. N. Miller, et al. 2019. Thymic regulatory T cells arise via two distinct developmental programs. *Nat. Immunol.* 20: 195–205.
26. Vernachio, J., M. Li, A. D. Donnenberg, and M. J. Soloski. 1989. Qa-2 expression in the adult murine thymus. A unique marker for a mature thymic subset. *J. Immunol.* 142: 48–56.
27. Wilson, A., L. M. Day, R. Scollay, and K. Shortman. 1988. Subpopulations of mature murine thymocytes: properties of $CD4^{-}CD8^{+}$ and $CD4^{+}CD8^{-}$ thymocytes lacking the heat-stable antigen. *Cell. Immunol.* 117: 312–326.
28. Azzam, H. S., A. Grinberg, K. Lui, H. Shen, E. W. Shores, and P. E. Love. 1998. CD5 expression is developmentally regulated by T cell receptor (TCR) signals and TCR avidity. *J. Exp. Med.* 188: 2301–2311.
29. Azzam, H. S., J. B. DeJarnette, K. Huang, R. Emmons, C. S. Park, C. L. Sommers, D. El-Khoury, E. W. Shores, and P. E. Love. 2001. Fine tuning of TCR signaling by CD5. *J. Immunol.* 166: 5464–5472.
30. Fulton, R. B., S. E. Hamilton, Y. Xing, J. A. Best, A. W. Goldrath, K. A. Hogquist, and S. C. Jameson. 2015. The TCR's sensitivity to self peptide-MHC dictates the ability of naive $CD8^{+}$ T cells to respond to foreign antigens. *Nat. Immunol.* 16: 107–117.
31. Lo, W. L., M. Kuhlmann, G. Rizzuto, H. A. Ekiz, E. M. Kolawole, M. P. Revelo, R. Andargachew, Z. Li, Y. L. Tsai, A. Marson, et al. 2023. A single-amino acid substitution in the adaptor LAT accelerates TCR proofreading kinetics and alters T-cell selection, maintenance and function. *Nat. Immunol.* 24: 676–689.
32. Tai, X., M. Cowan, L. Feigenbaum, and A. Singer. 2005. CD28 costimulation of developing thymocytes induces Foxp3 expression and regulatory T cell differentiation independently of interleukin 2. *Nat. Immunol.* 6: 152–162.
33. Jenkins, M. K., P. S. Taylor, S. D. Norton, and K. B. Urdahl. 1991. CD28 delivers a costimulatory signal involved in antigen-specific IL-2 production by human T cells. *J. Immunol.* 147: 2461–2466.
34. Norton, S. D., L. Zuckerman, K. B. Urdahl, R. Shefner, J. Miller, and M. K. Jenkins. 1992. The CD28 ligand, B7, enhances IL-2 production by providing a costimulatory signal to T cells. *J. Immunol.* 149: 1556–1561.
35. Burchill, M. A., J. Yang, C. Vogtenhuber, B. R. Blazar, and M. A. Farrar. 2007. IL-2 receptor beta-dependent STAT5 activation is required for the development of $Foxp3^{+}$ regulatory T cells. *J. Immunol.* 178: 280–290.
36. Fontenot, J. D., J. P. Rasmussen, M. A. Gavin, and A. Y. Rudensky. 2005. A function for interleukin 2 in Foxp3-expressing regulatory T cells. *Nat. Immunol.* 6: 1142–1151.
37. Lio, C. W., and C. S. Hsieh. 2008. A two-step process for thymic regulatory T cell development. *Immunity* 28: 100–111.
38. Owen, D. L., S. A. Mahmud, K. B. Vang, R. M. Kelly, B. R. Blazar, K. A. Smith, and M. A. Farrar. 2018. Identification of cellular sources of IL-2 needed for regulatory T cell development and homeostasis. *J. Immunol.* 200: 3926–3933.
39. Hemmers, S., M. Schizas, E. Azizi, S. Dikiy, Y. Zhong, Y. Feng, G. Altan-Bonnet, and A. Y. Rudensky. 2019. IL-2 production by self-reactive CD4 thymocytes scales regulatory T cell generation in the thymus. *J. Exp. Med.* 216: 2466–2478.
40. Brown, J. A., D. M. Dorfman, F. R. Ma, E. L. Sullivan, O. Munoz, C. R. Wood, E. A. Greenfield, and G. J. Freeman. 2003. Blockade of programmed death-1 ligands on dendritic cells enhances T cell activation and cytokine production. *J. Immunol.* 170: 1257–1266.
41. Oh, J., N. Wu, A. J. Barczak, R. Barbeau, D. J. Erle, and J. S. Shin. 2018. CD40 mediates maturation of thymic dendritic cells driven by self-reactive $CD4^{+}$ thymocytes and supports development of natural regulatory T cells. *J. Immunol.* 200: 1399–1412.
42. Ishida, M., Y. Iwai, Y. Tanaka, T. Okazaki, G. J. Freeman, N. Minato, and T. Honjo. 2002. Differential expression of PD-L1 and PD-L2, ligands for an inhibitory receptor PD-1, in the cells of lymphohematopoietic tissues. *Immunol. Lett.* 84: 57–62.
43. Francisco, L. M., V. H. Salinas, K. E. Brown, V. K. Vanguri, G. J. Freeman, V. K. Kuchroo, and A. H. Sharpe. 2009. PD-L1 regulates the development, maintenance, and function of induced regulatory T cells. *J. Exp. Med.* 206: 3015–3029.

44. Wang, L., K. Pino-Lagos, V. C. de Vries, I. Guleria, M. H. Sayegh, and R. J. Noelle. 2008. Programmed death 1 ligand signaling regulates the generation of adaptive Foxp3^{+}CD4^{+} regulatory T cells. *Proc. Natl. Acad. Sci. U. S. A.* 105: 9331–9336.
45. Tai, X., A. Indart, M. Rojano, J. Guo, N. Apenes, T. Kadakia, M. Craveiro, A. Alag, R. Etzensperger, M. E. Badr, et al. 2023. How autoreactive thymocytes differentiate into regulatory versus effector CD4^{+} T cells after avoiding clonal deletion. *Nat. Immunol.* 24: 637–651.
46. Lim, T. S., V. Chew, J. L. Sieow, S. Goh, J. P. Yeong, A. L. Soon, and P. Ricciardi-Castagnoli. 2016. PD-1 expression on dendritic cells suppresses CD8^{+} T cell function and antitumor immunity. *Oncoimmunology* 5: e1085146.
47. Chikuma, S., S. Terawaki, T. Hayashi, R. Nabeshima, T. Yoshida, S. Shibayama, T. Okazaki, and T. Honjo. 2009. PD-1-mediated suppression of IL-2 production induces CD8+ T cell anergy in vivo. *J. Immunol.* 182: 6682–6689.